

THE EFFECT OF AREA VARIATION ON WAVE ROTOR ELEMENTS

Jack Wilson
NYMA, Inc.
Brook Park, Ohio 44142

SUMMARY

The effect of varying the cross-sectional flow area of the passages of a wave rotor is examined by means of the method of characteristics. An idealized expansion wave, an idealized inlet port, and an idealized compression stage are considered. It is found that area variation does not have a very significant effect on the expansion wave, nor on the compression stage. For the expansion wave, increasing the passage area in the flow direction has the same effect as a diffuser, so that the flow emerges at a lower velocity than it would for the constant area case. This could be advantageous. The inlet is strongly affected by the area variation, as it changes the strength of the hammer shock wave, thereby changing the pressure behind it. In this case, reduction in the passage area in the flow direction leads to increased pressure. However this result is dependent on the assumption that the inlet conditions remain constant with area variation. This may not be the case.

NOMENCLATURE

$A(x)$	area of a passage at location x
$a, a(i,j)$	speed of sound
B	coefficient of area variation defined in equations (2) and (3)
$h(x)$	passage height at location x
i	index for Q waves
j	index for P waves
M	flow Mach number
M_h	Mach number of hammer shock
$P, P(i,j)$	Riemann variable travelling at velocity $(u + a)$
p	pressure
$Q, Q(i,j)$	Riemann variable travelling at velocity $(u - a)$
S	Mach number function defined in equation (13)
T	temperature
$t(i,j)$	dimensionless time at intersection of i th Q wave and j th P wave
U_h	velocity of hammer shock wave

$u(i,j)$ flow velocity at intersection of i th Q wave and j th P wave

$x,x(i,j)$ dimensionless position along a passage

γ ratio of specific heats

Subscripts

a value in front of a shock wave

b value behind a shock wave

f final, mixed-out, stagnation value

0 inlet stagnation value, or value in initial, at rest, region prior to expansion, and prior to compression

1 value in inlet port

2 value in port 2

3 stagnation value in port 3

4 value in port 4

wall value at closed end of a passage

INTRODUCTION

Pressure exchange wave rotors normally have constant area passages. However, a reduction in area, combined with a flow deflection, at the downstream end of a passage has been investigated by Weber (1991) for a wave turbine. The resulting increased exit tangential momentum could lead to more power being generated. Analysis indicated that this was not the case. Pfeifer and Garlich (1990) claimed that the use of passages having an exit area smaller than the entrance area could increase the performance of a "pressure wave machine," i.e. wave rotor, intended for use as a turbocharger for an internal combustion engine. With distance x measured from exit to entry, and using the relation for the passage height:

$$h(x) = h(0) + 0.2x^2 \quad (1)$$

they found that the compression efficiency increased to 92.6 percent, from 92.1 percent for a machine with constant area. The overall efficiency increased from 50.2 percent for a constant area machine to 52.4 percent. No reason for these increases in efficiency was given, nor was it stated whether these results were theoretical or experimental. It is clear that the device that they were considering is similar to, or is, the COMPREX[®], developed by Brown-Boveri. The COMPREX uses a reverse-flow cycle, in which air enters and leaves from the same, entry, side of the rotor, and exhaust gas enters and leaves from the opposite, or exit, side.

At the NASA Lewis Research Center, work on wave rotors is aimed at providing a topping cycle for gas turbines (Wilson and Paxson, 1996, Welch, Jones and Paxson 1995). For this application, effort has principally centered on the through-flow cycle (Welch, 1996). The wave diagram of a through-flow cycle that might be used for this application is shown in figure 1. In this cycle, air enters port 1 from one side, is compressed, and passes out of the other side of the rotor at port 2. This compressed air is then heated, and returned back into the rotor on the inlet side, at port 3. It expands, and finally emerges on the outlet side, at port 4. This cycle is thus quite different from the cycle used in the COMPREX, and conclusions reached about the COMPREX may not be correct for this cycle. It is therefore worthwhile examining the effect of area variation on the through-flow cycle. In this paper, the method of

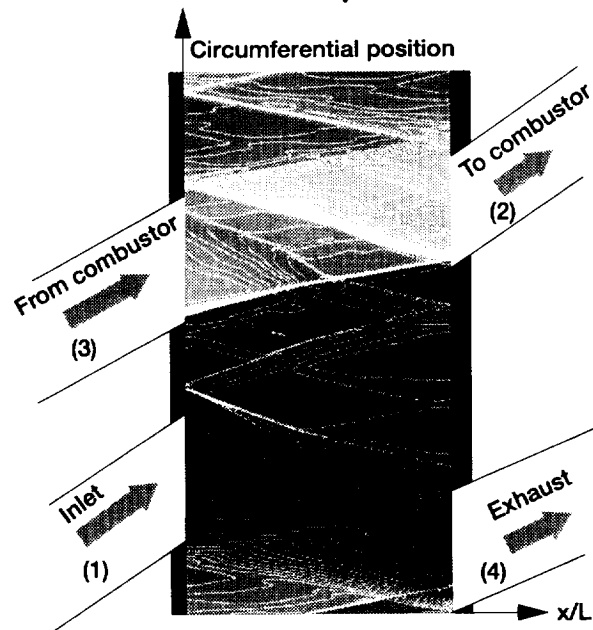


Figure 1.—The wave diagram for a four-port wave rotor cycle. The contour lines are isobars. This diagram, courtesy of D. Paxson, was calculated using the NASA Lewis one-dimensional CFD code for wave rotors (Paxson, 1995).

characteristics is used to assess the effects of area variation on portions of the cycle. It is assumed that the area change takes place without change in the mean radius; in other words, centrifugal effects are not considered.

METHODOLOGY

The cycle shown in figure 1 can be thought of as having three elements. These are (1) the expansion wave, at the lower right of figure 1, which is generated when a passage is suddenly opened to the exhaust port 4, (2) the charging portion consisting of the inlet port 1 (lower left), and the hammer shock which brings entering air to rest, and (3) the compression region in which gas returning to the rotor from the burner through port 3 drives a shock wave into the air on board the rotor, causing it to exit at port 2. Each of these elements will be treated separately, using ideal models of each one.

The Expansion Wave

The expansion wave is shown in figure 2. The expansion wave occurs when a passage, containing fluid at rest, is opened to the exhaust port 4 at its downstream end, by rotation of the passage into the port region. The fluid in the passage is at higher pressure than that in the port, so an expansion wave travels upstream in order to exhaust the passage. The expansion reflects off the wall at the upstream end of the passage, and returns to the exhaust port 4. When it reaches the port, it reduces the velocity of the fluid leaving the passage. Ideally, the port is closed when the relative velocity is reduced to zero. In the model of the expansion wave, it is assumed that the fluid in the passage before the port opens is completely at rest, relative to the rotor, and uniform in density and pressure. This will not be the case in a real cycle. Also the passage will be assumed to open, and close, to the port instantaneously, which is obviously impossible.

The method of characteristics for unsteady flow has been described very well by Rudinger (1955). In particular, Rudinger gives the discharge of a pressurized duct of constant area which is suddenly opened to a lower pressure, as an example (page 186). This is exactly the same case as the expansion in a wave rotor, and the technique for calculating it is the same. In the present work, the only difference is that instead of drawing the wave diagram, a computer

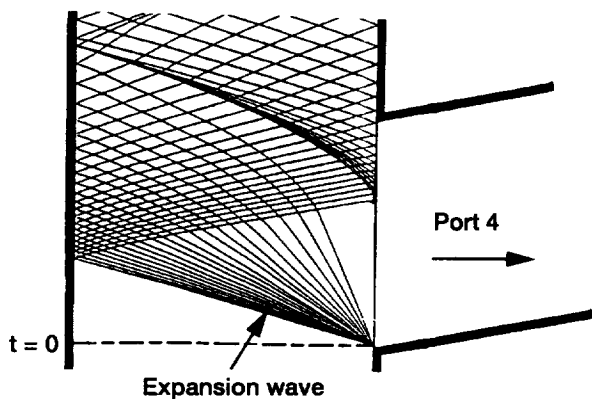


Figure 2.— A calculation of the expansion wave using the method of characteristics. The lines inclined to the left are lines of constant Q (for constant area), which have a slope of $a_0/(u-a)$. The lines inclined to the right are lines of constant P (for constant area), which have a slope of $a_0/(a+u)$.

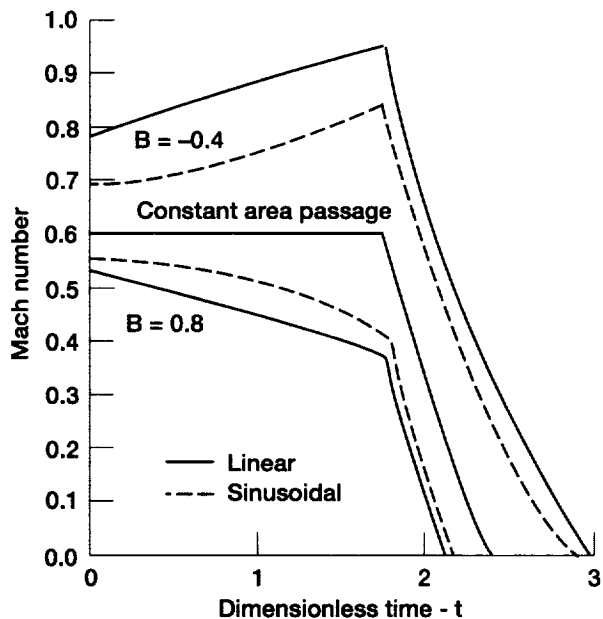


Figure 3.—Mach number distributions in the outlet port 4 as generated by the expansion wave. The port is closed when the velocity falls to zero.

was programmed to calculate it. The resulting wave diagram, again for a constant area passage, is given in figure 2, and the port Mach number distribution is given in figure 3.

For the case in which area varies along the passage, it is necessary to specify the area variation. Two cases were examined: a linear variation, i.e.;

$$A(x) = A(0).(1 + Bx) \quad (2)$$

and a sinusoidal variation, namely,

$$A(x) = A(0).(1 + B\sin(\pi x/2)) \quad (3)$$

In the method of characteristics, the Riemann variables, P and Q, which convect along waves travelling at velocity $(a + u)$, and $(a - u)$ respectively are calculated at successive points in the flow. In the present scheme, P waves are given an index j, and Q waves an index i. Each new point, located at $x(i,j)$, $t(i,j)$ is derived from known points $x(i-1,j)$, $t(i-1,j)$ and $x(i,j-1)$, $t(i,j-1)$, as illustrated in figure 4. From the point $x(i-1,j)$, $t(i-1,j)$ a line is drawn with slope

$$dt/dx = a_0/(a(i-1,j) + u(i-1,j)) \quad (4)$$

This is the P wave, shown as a dashed line in figure 4. Similarly, the Q wave is drawn (chain-dotted) from point $x(i,j-1)$, $t(i,j-1)$ with slope;

$$dt/dx = a_0/(a(i,j-1) - u(i,j-1)) \quad (5)$$

Where the two lines cross is the location of the new point. In the case of constant area, isentropic flow with no body forces or sideways leakage, P and Q are constant along each wave, so that at the new point;

$$P(i,j) = P(i-1,j) \quad (6)$$

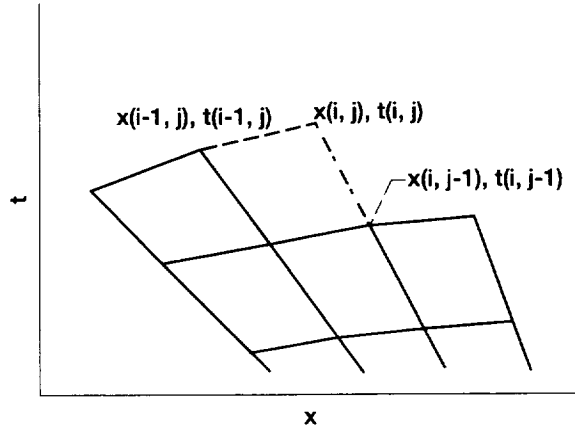


Figure 4.—Diagram illustrating how the method of characteristics calculation is performed.

$$Q(i, j) = Q(i, j - 1) \quad (7)$$

Thus P and Q are known at the new point, and u and a are derived from these values.

When there is area variation, the values of P and Q change as the wave propagates along the passage (Rudinger, p. 33). The change in P in going from $x(i - 1, j)$ to $x(i, j)$ is given by;

$$dP = -\frac{au}{(a + u)} \ln(A(x(i, j))/A(x(i - 1, j))) \quad (8)$$

and the change in Q in going from $x(i, j-1)$ to $x(i, j)$ is

$$dQ = -\frac{au}{(a - u)} \ln(A(x(i, j-1))/A(x(i, j))) \quad (9)$$

so that the values of P and Q at $x(i, j)$ will be

$$P(i, j) = P(i - 1, j) + dP \quad (10)$$

$$Q(i, j) = Q(i, j - 1) + dQ \quad (11)$$

from which a and u are calculated at $x(i, j), t(i, j)$. This scheme is not the same as that proposed by Rudinger for handling area variation, but is more accurate, and more easily amenable to computer calculation. Rudinger proposed replacing the continuous area variation by a set of discrete step changes in area.

The result of the calculation by the method of characteristics is the velocity distribution of the flow at the exhaust port, for a given value of expansion ratio. The expansion ratio is the ratio of pressure in the exhaust port to pressure in the passage before it opens to the exhaust port. The distribution of velocity at port 4 is nonuniform. The flow will mix to form a uniform velocity downstream. This constant area mixing process results in loss of stagnation pressure. Calculation of this mixing has been described by Foa (1960), and provides the stagnation pressure, p_{4f} , stagnation temperature, T_{4f} , and Mach number of the uniform flow. With the final stagnation pressure and temperature known, the adiabatic expansion efficiency can be calculated, i.e.

$$\eta = (1 - T_{4f}/T_o) / (1 - (p_{4f}/p_o)^{(\gamma-1)/\gamma})$$

The Inlet Port

The expansion wave creates a low pressure at the upstream end of each passage, so that when the passage is exposed to the inlet port, the inlet air is ingested into the passage, and all the gas in the passage is moving towards the exhaust port. When the exhaust port closes, this gas must be brought to rest, which is accomplished by means of a shock wave which travels upstream. A simplified model of this process will be assumed for calculating the effect of area variation. This model will be a duct with steady flow through it, which is suddenly closed at the downstream end, so that a shock wave, called a hammer shock, propagates upstream to stop the flow. This is equivalent to the situation at the end of a shock tube, in which the incident shock is reflected as a shock of sufficient strength to bring the flow to rest. For a constant area duct, this case can be solved analytically quite simply. The Mach number of the hammer shock wave, M_h , is given by

$$M_h = \sqrt{S} + \sqrt{(S+1)} \quad (12)$$

where

$$S = ((\gamma + 1)M/4)^2 \quad (13)$$

and M is the Mach number of the flow in the duct upstream of the reflected shock wave.

When the duct changes area, the strength of the hammer shock will alter as it propagates upstream. Kantrowitz (1958) has given an expression for the speed of a shock wave in laboratory coordinates, which can be rewritten in terms of Riemann variables, for a Q shock, as;

$$U_h = 0.5(P_a - Q_a) + (\gamma + 1)(Q_a - Q_b + \text{del } P)/8 - ((\gamma - 1)/4)(P_a + Q_a) \sqrt{1 + ((\gamma + 1)(Q_a - Q_b + \text{del } P)/(2(\gamma - 1)(P_a + Q_a)))^2} \quad (14)$$

where $\text{del } P = P_b - P_a$.

Thus if P_a , Q_a , and Q_b are known, the shock strength is fixed, and everything is known at that point. This may not seem obvious from the above equation, since $\text{del } P$ appears unknown. However $\text{del } P$ is small for a Q shock, and actually is a function of $(Q_b - Q_a)$, (see Kantrowitz) so it is known. This forms the basis of the calculation. The steady flow in the duct is known, so P_a and Q_a can be calculated at each value of x . The duct is suddenly closed at the downstream end, and the initial value of the hammer shock strength can be found from equation (12) above. The shock will propagate upstream at the known speed, so that the time at which it arrives at a selected value of x can be found. From this point, a Q wave can be projected backwards in time to the closed end, and a P wave from this point back to the shock, as shown in figure 5. At the shock, the values of P_a and Q_a can be interpolated, and since the strength is known, P_b can be found. With P_b determined, the value of P_{wall} can be found using equations (8) and (10). Since the flow must be at rest at the wall, $Q_{\text{wall}} = P_{\text{wall}}$. The value of Q_b at the position x follows using equations (9) and (11). Thus P_a , Q_a , and Q_b are known at x , and the shock speed can be calculated with equation (14). The process is repeated until the shock wave reaches the upstream end of the passage. The pressure behind the shock is calculated at each position of the shock, and the final volume-averaged pressure is;

$$\bar{p}_b = \int_0^1 p_b(x)A(x)dx / \int_0^1 A(x)dx \quad (15)$$

This is taken as the measure of the effectiveness of the charging element, i.e. the higher the average pressure, the more effective is the charging process. In similar fashion, an average temperature behind the shock can be calculated. Then a compression efficiency for the charging process can be defined as:

$$\eta = \left[\left(\bar{p}_b / p_o \right)^{(\gamma-1)/\gamma} - 1 \right] / \left[\bar{T}_b / T_o - 1 \right] \quad (16)$$

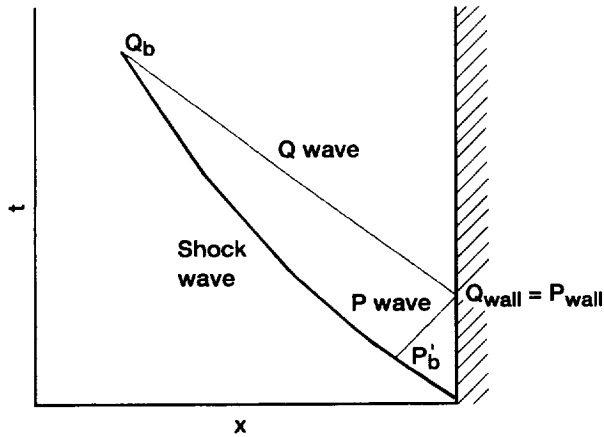


Figure 5.—Diagram showing how, in the calculation of the hammer shock wave, the value of Q_b at a new shock position is derived from the value of P_b at an earlier time.

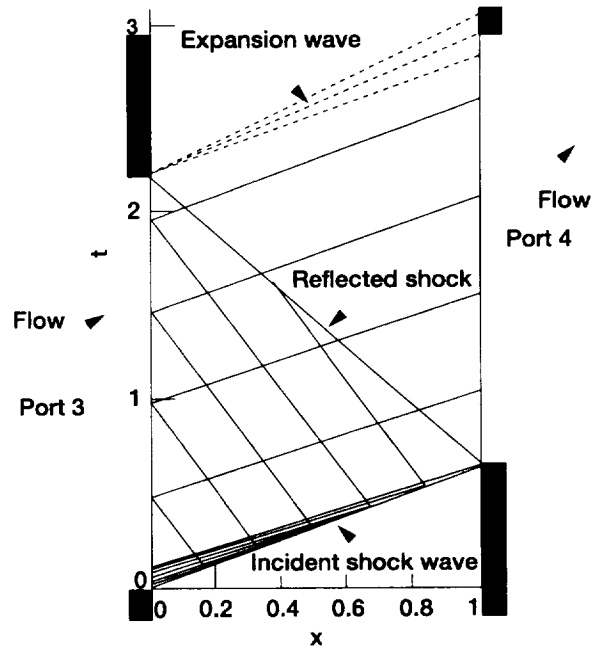


Figure 6.—A schematic diagram of the idealized upper portion of the cycle, showing the characteristics.

The Compression Stage

The upper portion of the cycle consists of the return port 3 on the left, and the exit port 2 on the right. Gas re-entering the wave rotor at port 3 from the burner drives a shock wave through the air in the passage, compressing it, and accelerating it to the right. The shock wave is reflected at port 2, travelling back upstream, and further compressing the air. The compressed air exits port 2. In the simplified model of the compression stage, shown in figure 6, the air in the passage is assumed to be uniform, and at rest, before the passage is opened to port 3. No interface is included between hot gas entering port 3, and cold gas in the passage; the pressure of the incoming gas is simply made high enough to drive a shock of the desired strength. The boundary condition for Q waves reaching port 3 is that the incoming stagnation pressure is constant.

The calculation is similar to that for the hammer shock. First the P shock is calculated. For this shock, P_a and Q_a are equal and constant everywhere, since the air in the passage was assumed to be at rest. When extrapolating back from behind the shock, the value of P calculated at port 3 is given by;

$$P = ((3 - \gamma)/(\gamma + 1))Q + \sqrt{16a_3^2/(\gamma^2 - 1) - 8((\gamma - 1)/(\gamma + 1)^2)Q^2} \quad (17)$$

This is the constant stagnation pressure boundary condition.

It is now necessary to calculate the grid of characteristics behind this shock wave in order to be able to find P_a and Q_a for the reflected shock wave. For the reflected shock wave, the back extrapolated P and Q waves meet at port 2, instead of at a wall as was the case for the hammer shock calculation. At an exit port, the boundary condition is constant static pressure. The shock waves are relatively weak, so that very little entropy is generated. Consequently, the isentropic constant pressure condition, namely $a_2 = \text{constant}$, can be applied. The relation between P and Q at the port is then:

$$Q = 4a_2/(\gamma + 1) - P \quad (18)$$

The characteristics calculation provides the pressure and velocity distribution at port 2. The velocity distribution can be quite nonuniform, particularly when there is area change. Consequently a mixing calculation is again used to find the final stagnation temperature and stagnation pressure, and hence compression efficiency, which is defined as:

$$\eta = \left[(p_{2f}/p_o)^{(\gamma-1)/\gamma} - 1 \right] / \left[T_{ef}/T_o - 1 \right] \quad (19)$$

RESULTS

The Expansion Wave

The results of the calculations for the expansion wave are given in table 1(a) for the linear change in area, and in table 1(b) for the sinusoidal variation in area with $\gamma = 1.4$. The calculation was carried out for a constant value of the ratio of final relative stagnation temperature to initial temperature of 0.85. This is approximately the smallest value possible for this ratio, since any lower value will result in Mach numbers of unity in the expanded flow. The mass fraction represents how much of the mass of air in the passage initially exits via the expansion wave. The expansion ratio is the ratio of static pressure in the exhaust port to the initial pressure (p_4/p_o). Note that the expansion ratio had to be altered as the area was varied in order to maintain a constant temperature ratio. The stagnation pressure is calculated assuming that the initial pressure in the passage is unity. It will be seen that the relative stagnation pressure increases slightly with increasing downstream area. The final mixed-out Mach number decreases simultaneously. However there is very little change in efficiency. Thus the main effect of area increase seems to be that the passage is acting as a diffuser. This could be beneficial.

The results with a sinusoidal area variation are not much different from those with a linear area variation, except that the sinusoidal change seems to be a less efficient diffuser. Area decrease is not favorable, as it causes the final Mach number to increase, and the efficiency and the mass fraction to decrease. Although area increase is apparently advantageous, diffuser losses, which have not been included here, will probably eliminate any gain in efficiency. Mach number distributions in the exit port are shown in figure 3 for both the linear area variation, and the sinusoidal area variation.

TABLE I.—THE EFFECT OF CHANGING PASSAGE AREA ON AN EXPANSION AT A CONSTANT VALUE OF THE RATIO OF EXPANDED, MIXED-OUT, STAGNATION TEMPERATURE TO INITIAL PASSAGE TEMPERATURE = 0.85

(a) Linear passage area variation ($A(x) = A(0)(1 + Bx)$)					
Coefficient B	Expansion efficiency	Expansion ratio	Discharge mass fraction	Relative total pressure ratio	Mixed-out Mach number
-0.4	0.941	0.362	0.630	0.545	0.588
-2	.975	.422	.625	.557	.536
0	.985	.451	.621	.561	.491
2	.989	.468	.618	.562	.458
4	.991	.479	.615	.563	.434
6	.991	.487	.612	.563	.415
8	.991	.492	.610	.563	.400

(b) Sinusoidal passage area variation ($A(x) = A(0)(1 + B \sin(\pi x/2))$)					
Coefficient B	Expansion efficiency	Expansion ratio	Discharge mass fraction	Relative total pressure ratio	Mixed-out Mach number
-0.4	0.960	0.403	0.583	0.552	0.542
-2	.979	.434	.604	.559	.515
0	.985	.451	.621	.561	.491
2	.988	.462	.635	.562	.473
4	.990	.469	.646	.563	.459
6	.990	.474	.656	.563	.448
8	.990	.477	.664	.563	.440

The Inlet Port

It was assumed that the inlet duct has an axial Mach number of 0.5. This is a typical value for proposed applications. The final averaged pressure is plotted as a function of the area coefficient B in figure 7 for both the linear area variation and the sinusoidal area variation. It will be seen that area variation has a significant effect on the final pressure, with a reduction in area resulting in a pressure increase. This is because the area reduction causes the flow to speed up at the downstream end of the passage, thus requiring a stronger shock to stop the flow. However, this is a consequence of assuming constant conditions at the inlet port. If this increase is to be realized, the cycle must produce the lower pressure required to accelerate the flow to the higher Mach number. There is little difference between the results for a linear area variation and those for a sinusoidal area variation. A sinusoidal area variation does result in a slightly higher final pressure, but the extra pressure hardly seems worth the complication of having to produce a more complicated passage shape.

The shock trajectory is plotted in figure 8 for the constant area case, and for the extreme area coefficients considered here, namely $B = 0.8$ and $B = -0.25$. The area variation causes a difference in the time at which the hammer shock reaches the trailing edge of the inlet port, so that the timing of the cycle will change with area variation. Since the mass flow into the port will be proportional to the time that the port is open, it will increase as the downstream area is reduced.

The Compression Stage

The conditions chosen for the compression stage were $a_3/a_0 = 1.2$, and $a_2/a_0 = 1.223$, with $\gamma = 1.4$. These values resulted in a primary shock Mach number of 1.52, and a reflected shock Mach number of 1.19 for the constant area case. The corresponding pressure ratios are 2.5 and 1.4 respectively, giving an overall stagnation pressure ratio of 4. This ratio is appropriate for a cycle that might be used in practise. The results are given in table 2(a) for the linear area variation, and table 2(b) for the sinusoidal area variation. As the area was varied, it was necessary to alter the value of a_2 to maintain a constant value of the stagnation temperature ratio. There is very little change in either final stagnation pressure, or efficiency, although what change there is suggests that increasing the area at the downstream end is advantageous, contrary to the result of Pfeifer and Garlich. The mass fraction, which is the fraction of the air which is initially in the passage that exits port 2, does change. The mass fraction has a maximum at constant area for the linear area variation, and at $B = 0.2$ for the sinusoidal area variation. The value of the mass fraction is greater than unity, indicating that gas from port 3 is entering port 2. However, this result may be a consequence of the very simplified model used for the compression stage.

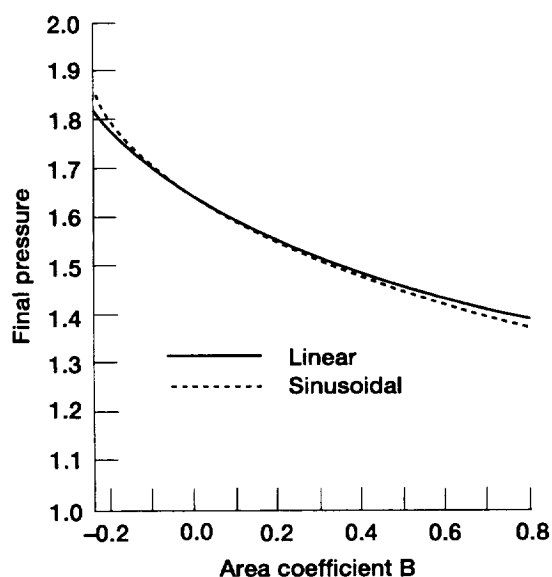


Figure 7.—The final averaged pressure produced by the hammer shock wave plotted against the area coefficient B .

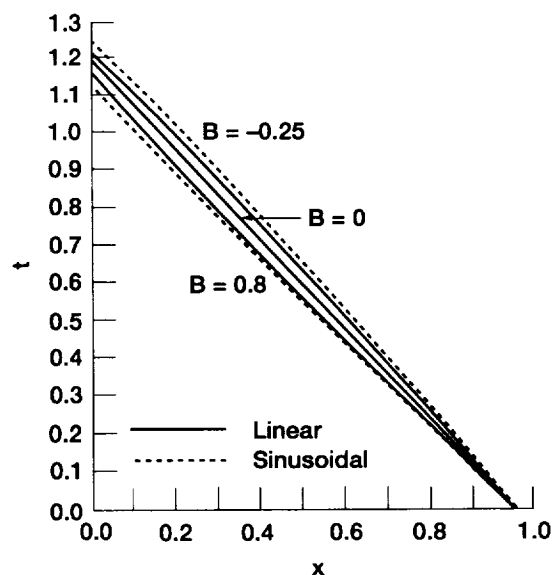


Figure 8.—The trajectories of the hammer shock wave for different values of the area coefficient B .

TABLE II.—THE EFFECT OF CHANGING PASSAGE AREA ON THE UPPER PORTION OF THE CYCLE AT A CONSTANT VALUE OF THE RATIO OF STAGNATION TEMPERATURE IN PORT 2 TO TEMPERATURE OF THE AIR INITIALLY IN THE PASSAGE = 1.525

(a) Linear area variation

Coefficient B	Compression efficiency	a_2	Discharge mass fraction	Relative total pressure ratio
-0.25	0.919	1218.8	2.07	3.968
-2	.921	1219.6	2.14	3.977
-.15	.922	1220.5	2.17	3.983
-.1	.923	1221.3	2.21	3.990
0	.925	1222.9	2.25	4.000
2	.925	1225.0	2.24	3.998
4	.926	1226.8	2.16	4.007
6	.926	1228.8	1.90	4.002
8	.924	1229.5	1.75	3.997

(b) Sinusoidal area variation

Coefficient B	Compression efficiency	a_2	Discharge mass fraction	Relative total pressure ratio
-0.25	0.915	1220.5	1.98	3.952
-2	.918	1221.0	2.06	3.967
-.15	.921	1221.5	2.12	3.976
-.1	.922	1222.0	2.18	3.987
0	.925	1222.9	2.25	4.000
2	.928	1224.2	2.30	4.013
4	.930	1226.5	2.11	4.026
6	.933	1229.7	1.65	4.036
8	.935	1231.4	1.37	4.048

CONCLUSIONS

Calculations using the method of characteristics show that variations in passage area do not greatly affect the efficiency or final stagnation pressure of either the expansion wave or the compression stage of the cycle, although area increase does act as a diffuser, resulting in the flow leaving the expansion at a lower Mach number. Area decrease has a significant effect in increasing the final pressure produced by the hammer shock on the incoming flow, and would seem to be the major effect of area variation. Whether this effect can actually be used in a real cycle will require complete cycle calculations. However, Pfeifer and Garlich claimed that area reduction increased the efficiency for the cycle they considered, so the present result is consistent with previous findings.

REFERENCES

- Foa, J.V., 1960, "Elements of Flight Propulsion," John Wiley & Sons, New York, NY.
- Kantrowitz, A., (1958), "One-Dimensional Treatment of Nonsteady Gas Dynamics," in Fundamentals of Gas Dynamics; edited by Emmons, H.W., Volume III of High Speed Aerodynamics and Jet Propulsion, Princeton University Press, Princeton, NJ, pp. 350-415.
- Paxson, D.E., 1995, "Comparison between numerically modelled and experimentally measured Wave-Rotor Loss Mechanisms," *Journal of Propulsion and Power*, Vol. 11, No. 5, pp. 908-914.
- Pfeifer, U. and Garlich, S., 1990, "Gasynamische Druckwellenmaschine mit nicht konstantem Zellenquerschnitt," German Patent No. DD 285 397 A5.
- Rudinger, G., 1955, "Wave Diagrams for Nonsteady Flow in Ducts," D. Van Nostrand Company, Inc., New York, NY.
- Weber, H.E., 1992, "Wave Engine Aerothermodynamic Design," *Journal of Engineering for Gas Turbines and Power*, Vol. 114, pp. 790-796.
- Welch, G.E., Jones, S.M., and Paxson, D.E., 1995, "Wave Rotor-Enhanced Gas Turbine Engines," AIAA 95-2799; also NASA TM-106998, and ARL-TR-806.
- Welch, G.E., 1996, "Two-Dimensional Computational Model for Wave Rotor Flow Dynamics", ASME Paper 96-GT-550; also NASA TM-107192, and ARL-TR-924.
- Wilson, J. and Paxson, D.E., 1996, "Wave Rotor Optimization for Gas Turbine Engine Topping Cycles." *Journal of Propulsion and Power*, Vol. 12, No. 4, pp. 778-785.

REPORT DOCUMENTATION PAGE

Form Approved
OMB No. 0704-0188

Public reporting burden for this collection of information is estimated to average 1 hour per response, including the time for reviewing instructions, searching existing data sources, gathering and maintaining the data needed, and completing and reviewing the collection of information. Send comments regarding this burden estimate or any other aspect of this collection of information, including suggestions for reducing this burden, to Washington Headquarters Services, Directorate for Information Operations and Reports, 1215 Jefferson Davis Highway, Suite 1204, Arlington, VA 22202-4302, and to the Office of Management and Budget, Paperwork Reduction Project (0704-0188), Washington, DC 20503.

1. AGENCY USE ONLY (<i>Leave blank</i>)		2. REPORT DATE July 1997	3. REPORT TYPE AND DATES COVERED Final Contractor Report	
4. TITLE AND SUBTITLE The Effect of Area Variation on Wave Rotor Elements			5. FUNDING NUMBERS WU-505-26-33 C-NAS3-27186	
6. AUTHOR(S) Jack Wilson				
7. PERFORMING ORGANIZATION NAME(S) AND ADDRESS(ES) NYMA, Inc. 2001 Aerospace Parkway Brook Park, Ohio 44142			8. PERFORMING ORGANIZATION REPORT NUMBER E-10784	
9. SPONSORING/MONITORING AGENCY NAME(S) AND ADDRESS(ES) National Aeronautics and Space Administration Lewis Research Center Cleveland, Ohio 44135-3191			10. SPONSORING/MONITORING AGENCY REPORT NUMBER NASA CR-202352	
11. SUPPLEMENTARY NOTES Project Manager, Larry Bober, Turbomachinery and Propulsion Systems Division, NASA Lewis Research Center, organization code 5810, (216) 433-3944.				
12a. DISTRIBUTION/AVAILABILITY STATEMENT Unclassified - Unlimited Subject Category 07 This publication is available from the NASA Center for AeroSpace Information, (301) 621-0390.			12b. DISTRIBUTION CODE	
13. ABSTRACT (<i>Maximum 200 words</i>) The effect of varying the cross-sectional flow area of the passages of a wave rotor is examined by means of the method of characteristics. An idealized expansion wave, an idealized inlet port, and an idealized compression stage are considered. It is found that area variation does not have a very significant effect on the expansion wave, nor on the compression stage. For the expansion wave, increasing the passage area in the flow direction has the same effect as a diffuser, so that the flow emerges at a lower velocity than it would for the constant area case. This could be advantageous. The inlet is strongly affected by the area variation, as it changes the strength of the hammer shock wave, thereby changing the pressure behind it. In this case, reduction in the passage area in the flow direction leads to increased pressure. However this result is dependent on the assumption that the inlet conditions remain constant with area variation. This may not be the case.				
14. SUBJECT TERMS Wave rotor; Wave rotor with area variation; Passage area variation			15. NUMBER OF PAGES 13	
			16. PRICE CODE A03	
17. SECURITY CLASSIFICATION OF REPORT Unclassified	18. SECURITY CLASSIFICATION OF THIS PAGE Unclassified	19. SECURITY CLASSIFICATION OF ABSTRACT Unclassified	20. LIMITATION OF ABSTRACT	